Spontaneous Symmetry Breaking of Acceptors in "Blue" Diamonds

Hyunjung Kim, A. K. Ramdas, and S. Rodriguez
Department of Physics, Purdue University, West Lafayette, Indiana 47907-1396

M. Grimsditch
Argonne National Laboratory, Argonne, Illinois 60439

T. R. Anthony
General Electric Company Corporate Research and Development, Schenectady, New York 12309
(Received 6 July 1999)

The electronic Raman transition between the lower $1s(p_{3/2})$ and the higher $1s(p_{1/2})$ state of a hole bound to a boron acceptor in diamond, examined under the high resolution of a Fabry-Pérot interferometer, reveals a doublet separated by (0.81 ± 0.15) cm^{-1}, indicative of a spontaneous symmetry breaking of the fourfold degenerate ground state. The *direct transition* between the levels into which $1s(p_{3/2}):\Gamma_8$ resolves, with a Raman shift of (0.80 ± 0.04) cm^{-1}, provides a remarkable confirmation of the symmetry lowering shown to arise from a static Jahn-Teller distortion.

PACS numbers: 71.55.Cn, 71.70.Ej, 78.30.Am

Viewed as a wide band gap semiconductor (band gap ~5.5 eV at room temperature), along with its combination of high electron and hole mobilities [1] as well as its exceptional thermal conductivity [2], diamond is currently under intense study for high temperature solid state electronics [3]. Basic studies of acceptors and donors are fundamental in the context of the physics of semiconductors. As point defects whose electronic structure can be theoretically formulated precisely in terms of the band structure of the host on the one hand and whose bound states can be explored with some of the most powerful spectroscopic techniques on the other, they have a unique position in the science of condensed matter.

A remarkable discovery was made by Custers in 1952 [4] who reported the occurrence of extremely rare diamond specimens having undetectable concentrations of nitrogen, the most common impurity in diamond, but with resistivities as low as a few Ω cm [5]. These specimens (classified as type IIb) display electrical conduction by free holes indicating that the impurities responsible for the low resistivity are acceptors. A systematic series of studies established that the substitutional group III boron is the acceptor in question [6]. Since these early investigations, boron has been successfully introduced in man-made diamonds, grown by the high-pressure–high-temperature (HPHT) technique as well as by chemical vapor deposition (CVD). In CVD growth, the isotopic composition is that of the gas (e.g., CH_4) used; thus one can obtain $^{12}C_{1-x}{}^{13}C_x$ diamonds with $0 \leq x \leq 1$. In addition, CVD growth combined with HPHT allows one to produce isotopically controlled single crystals of boron doped diamond [7].

Thanks to their successful incorporation in man-made and natural diamonds, to date the spectroscopic studies on dopants have necessarily been focused on substitutional boron acceptors. The Lyman transitions from the $1s$ ground state associated with the top of the valence band to the various p-like excited states have been reported by several investigators [8]. The evidence of bound states of a boron acceptor from the Lyman spectrum; its photoionization limit; Δ', the spin-orbit splitting of the $1s$ ground state corresponding to Δ, the spin-orbit splitting of the valence band maximum; the remarkable shift in the Lyman spectrum of ^{13}C diamond with respect to that of a specimen with composition reflecting the natural abundance of carbon [9], etc., are some of the highlights of its electronic structure. Type IIb diamonds are often intensely blue, a consequence of the absorption due to photoionization of holes bound to boron extending well into the red; the characteristic color of type IIb diamonds is due to the residual blue of the transmitted white light.

Recently we recognized that Raman spectroscopy [10,11] offers a splendid opportunity to discover the Raman allowed and infrared forbidden electronic transition at Δ' *between* the spin-orbit split ground states, $1s(p_{3/2}):\Gamma_8$ and $1s(p_{1/2}):\Gamma_7$ of boron acceptors in diamond [12]. Diamond with its unparalleled transparency and large scattering power is ideally suited for Raman spectroscopy. The bound states of acceptors in semiconductors are fully described in terms of the well-known effective mass theory of Kohn and Luttinger [13,14] incorporating the details of the valence band extremum along with Δ, its spin-orbit splitting (Fig. 1). The energy level scheme of the shallow acceptors, which become electrically neutral in substantial numbers upon cooling to helium temperatures, allows one to observe their Lyman excitations in the infrared and the Δ' line in the Raman spectrum. In Fig. 2, the inset shows the Stokes/anti-Stokes pair of the electronic Raman lines at Δ' as well as the Brillouin components generated by the inelastic light scattering from the long wavelength transverse acoustic (TA) and longitudinal acoustic (LA) phonons. These measurements were performed with a

 0031-9007/99/83(20)/4140(4)$15.00

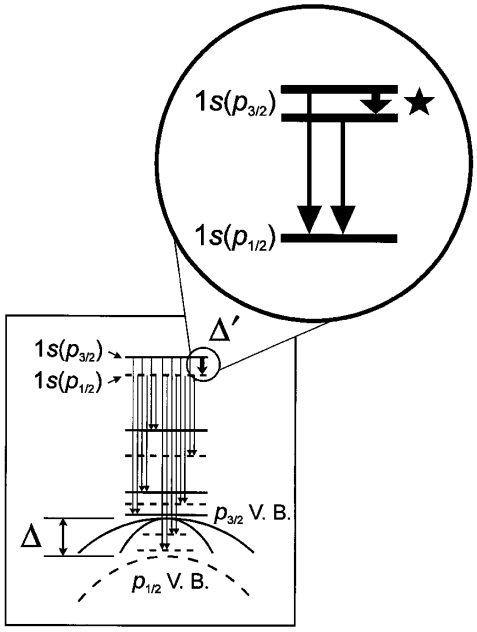

FIG. 1. Energy level scheme of a hole bound to a substitutional boron acceptor in diamond. The Jahn-Teller split $1s(p_{3/2})$ levels and the transition between them, identified with a star ($\star$), and the two transitions resulting in the Δ' line as a doublet are shown in the enlarged view presented within the circle. V. B.: valence band.

grating double monochromator aided by a tracking third monochromator.

When Δ' is examined under the high resolution of a multipassed, piezoelectrically scanned, tandem Fabry-Pérot interferometer [15], we discovered that it is actually a doublet with a separation of $0.81 \pm 0.15\ \mathrm{cm}^{-1}$, as shown in Fig. 2. We ensured that the doublet structure did not originate in the procedure adopted to mount the diamond specimens. Random strains introduced during the crystal growth are not expected to be homogeneous and the same from specimen to specimen, whereas our measurements on four distinct samples (two man-made and two natural) with the same natural isotopic composition show identical splittings.

An intrinsic lowering of the site symmetry of a point defect in which the new equilibrium position ensures that the decrease in the ground state electronic energy compensates the increase in elastic energy—the so-called static Jahn-Teller effect [16]—offers a natural explanation for our observation. We note that the $1s(p_{3/2})$ ground state of boron acceptors is fourfold degenerate; it belongs to the Γ_8 irreducible representation of $\overline{T}_d$, the site symmetry of boron before the lowering of symmetry. The Γ_8 level resolves into two Kramers doublets, one increasing and the other decreasing linearly in energy as a function of a parameter describing the symmetry lowering whereas such a distortion will produce an increased elastic energy quadratic in that parameter; the new equilibrium position is thus at a lower symmetry. This lowering of the symmetry can be expressed in terms of a distortion described by a set of coordinates $\{Q_i\}$ classified according to the symmetry of the acceptor site, more specifically, the irreducible representations of the group T_d. The deformation introduces a perturbation $H' = \sum_i V_i(\mathbf{r})Q_i + \sum_{i,j} V_{ij}(\mathbf{r})Q_iQ_j + \ldots$ where $V_i(\mathbf{r})$ and $V_{ij}(\mathbf{r})$ are potential functions depending on the hole position $\mathbf{r}$. Only coordinates Q_i belonging to either the Γ_3 or to the Γ_5 irreducible representation yield nonvanishing matrix elements of H' in the Γ_8 manifold. In the first case Q_1 and Q_2 generate Γ_3, while in the second, a different set of three coordinates generate Γ_5. For a Γ_3 deformation, the 4×4 matrix H' in the Γ_8 manifold is, to second order, of the form

$$H' = -V\{[Q_1 + \lambda(Q_1^2 - Q_2^2)](2J_z^2 - J_x^2 - J_y^2) + \sqrt{3}\,(Q_2 - 2\lambda Q_1 Q_2)\,(J_x^2 - J_y^2)\}, \qquad (1)$$

where V is a reduced matrix element of $V_1(\mathbf{r})$ and $V_2(\mathbf{r})$ (taken to be positive without loss of generality), λ is the ratio of the strength of the second order reduced matrix element to that of the first order (assumed less than unity), and J_x, J_y, and J_z are the angular momentum operators for $J = 3/2$ referred to the cubic axes, x, y, and z. The energy eigenvalues of H' are simple functions of Q_1 and Q_2, linear in Q_1 and Q_2 with small quadratic corrections. The lower level decreases with increasing $Q = (Q_1^2 + Q_2^2)^{1/2}$ and the balance of this decrease with the energy of deformation, quadratic in Q_1 and Q_2 determines the magnitudes of these coordinates as well as the energy separation of the Kramers doublets. Letting $Q_1 = Q\cos\varphi$ and $Q_2 = Q\sin\varphi$, the energy eigenvalues are $\pm 3VQ(1 + \lambda^2Q^2 + 2\lambda Q\cos 3\varphi)^{1/2}$; if $\lambda > 0 (\lambda < 0)$ the minimum of the energy occurs for $\varphi = 0, \pm 2\pi/3 (\varphi = \pi, \pm\pi/3)$; the eigenvectors are those of J_z^2 for $\varphi = 0$ labeled here $\psi_{\pm 3/2}$ and $\psi_{\pm 1/2}$ and, equivalently, for $\varphi = \pm 2\pi/3$ they are those of J_x^2 or J_y^2. For $\varphi = 0$ the lowest energy level corresponds to the states $\psi_{\pm 3/2}$ if $V > 0$ while the upper doublet is formed by $\psi_{\pm 1/2}$. The other cases lead to equivalent results. The choice in which V and λ have the same sign is consistent with the experimental relative intensities of the Δ' components whose interpretation follows.

In Fig. 3 we display the Jahn-Teller split Δ' doublet, recorded in the right-angle scattering geometry with incident light along $\mathbf{y} \| [010]$ and scattered along $\mathbf{z} \| [001]$. This geometry allows the incident light to be polarized along $\mathbf{z}$ or $\mathbf{x} \| [100]$ and the scattered beam to be analyzed along $\mathbf{y}$ or $\mathbf{x}$; the polarization combinations are indicated in the notation used to describe the four observations, e.g., $\mathbf{y}(\mathbf{zy})\mathbf{z}$ shows incident light to be along $\mathbf{y}$, polarized parallel to $\mathbf{z}$, and scattered along $\mathbf{z}$, while analyzed parallel to $\mathbf{y}$. The two components of the Δ' line display distinct relative intensities in the four polarization configurations. The theory outlined above predicts the ratios of the intensities of the low- to high-energy components of Δ' for the first three polarization configurations shown in Fig. 3 to be (a) 3:1 for ($\mathbf{zy}$); (b) 0:12 for ($\mathbf{xy}$); and (c) 3:1 for ($\mathbf{zx}$). In configurations (a), (b), and (c) the absolute intensities are proportional to γ_3^2, γ_3 being one of three Luttinger parameters [11]. In (d) for ($\mathbf{xx}$),

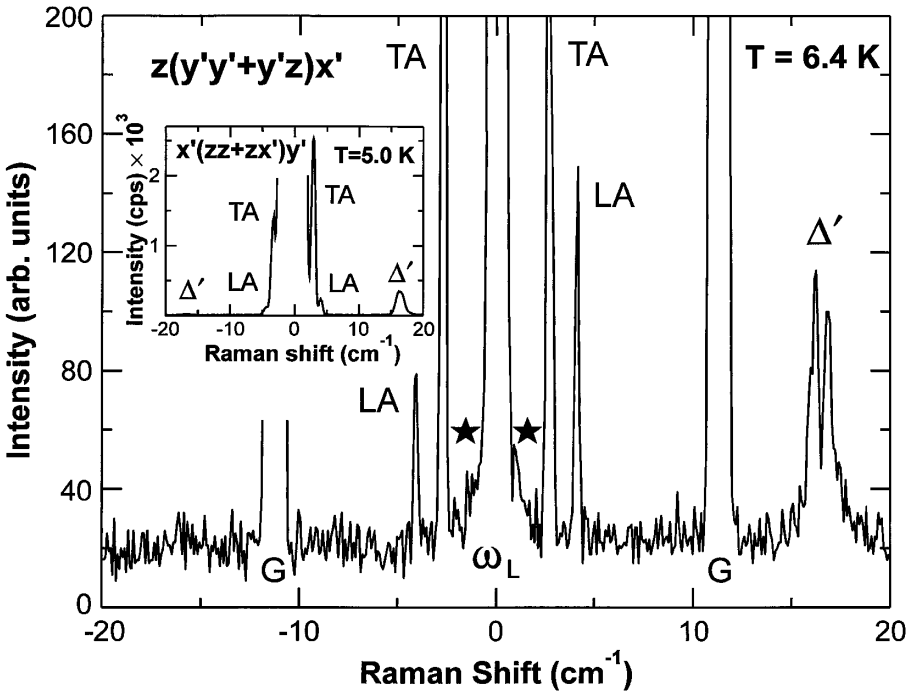

FIG. 2. The Δ' line as a Jahn-Teller doublet, the transition between the Jahn-Teller split $1s(p_{3/2})$ levels, labeled with a star ($\star$), and the intrinsic transverse acoustic (TA) and longitudinal acoustic (LA) Brillouin components in the scattered light from a natural type IIb diamond spectrally analyzed with a high resolution, multipassed, piezoelectrically scanned, tandem Fabry-Pérot interferometer. The spectrum is recorded in a right-angle scattering geometry $\mathbf{z}(\mathbf{y}'\mathbf{y}' + \mathbf{y}'\mathbf{z})\mathbf{x}'$; here $\mathbf{x}' \| [110]$, $\mathbf{y}' \| [\bar{1}10]$, and $\mathbf{z} \| [001]$ and the incident light along $\mathbf{z}$ is vertically polarized along $\mathbf{y}'$ whereas the scattered light along $\mathbf{x}'$ is not analyzed. The wavelength of the exciting laser radiation is 5145 Å (Ar^+) and 4765 Å (Ar^+) for the main figure and the inset, respectively. Temperature of measurement (T) is indicated in the figure. ω_L is the unshifted laser frequency and G identifies its "ghosts" due to leakage in the tandem operation. The unresolved Δ' doublet as it appears under the lower resolution of a double grating monochromator is shown in the inset; the spectrum is recorded in a right angle scattering geometry $\mathbf{x}'(\mathbf{zz} + \mathbf{zz}')\mathbf{y}'$. cps: counts per second.

while the theoretical ratio is 1:3, the absolute intensities are proportional to γ_2^2, where the Luttinger parameter γ_2 has been shown to be 1 order of magnitude smaller than γ_3. We note that the low energy component of Δ' in $(\mathbf{xy})$ is forbidden; whether it owes its appearance to a leakage associated with the finite collection angle in the scattered light or to the accidental birefringence diamond specimens sometimes exhibit or to higher order admixture of $\psi_{\pm 1/2}$ with $\psi_{\pm 3/2}$ is yet to be determined.

We have also explored the consequences of a Jahn-Teller distortion with Γ_5 symmetry. While a Jahn-Teller splitting of the $1s(p_{3/2})$ into a doublet does occur, the intensity of each component is equal to that of the other in every polarization configuration displayed in Fig. 3. This is contrary to the experimental findings discussed above.

The alternate point of view of the dynamic Jahn-Teller effect is again difficult to reconcile with the experimental findings. Considering Γ_3 phonons in conjunction with the $1s(p_{3/2})$:Γ_8, it can be readily seen that it will result in $\Gamma_6 + \Gamma_7 + \Gamma_8$ vibronic states; similarly, $1s(p_{1/2})$:Γ_7 and Γ_3 phonons together produce a Γ_8 vibronic state. Once again, the relative intensities of the Jahn-Teller components (even if forced to be only two) cannot conform to the results in Fig. 3. Similar remarks apply to vibronic states involving Γ_5 phonons.

An alternative model like that in Matsumoto *et al.* [17] for boron acceptors in 6H-SiC cannot be reconciled with the polarization characteristics in Fig. 3.

It is significant to note that in Figs. 2 and 3 the unshifted laser line at ω_L is flanked on either side with a signature, identified with a star ($\star$), having a shift of 0.80 ± 0.04 cm^{-1}. This shift is, within experimental uncertainties, identical to the spacing of the Jahn-Teller doublet. In other words, the star transitions are the Stokes/anti-Stokes pair of Raman transitions *between* the Jahn-Teller components of the Γ_8 level shown in the enlarged view in the circle displayed in Fig. 1. This is one of the smallest Raman shifts ever reported in the literature other than those of Brillouin components.

We draw attention to the several "well resolved doublets" in the photoluminescence and photoluminescence excitation spectra of excitons bound to Al, Ga, and In acceptors in Si reported by Karasyuk *et al.* [18] and ascribed to a Jahn-Teller splitting of the neutral acceptor ground state. The simplicity of a neutral acceptor by itself rather than in conjunction with an exciton and the rich detail available in the Raman spectra via the polarization configurations as demonstrated in the present study provide a convincing case for a Jahn-Teller effect.

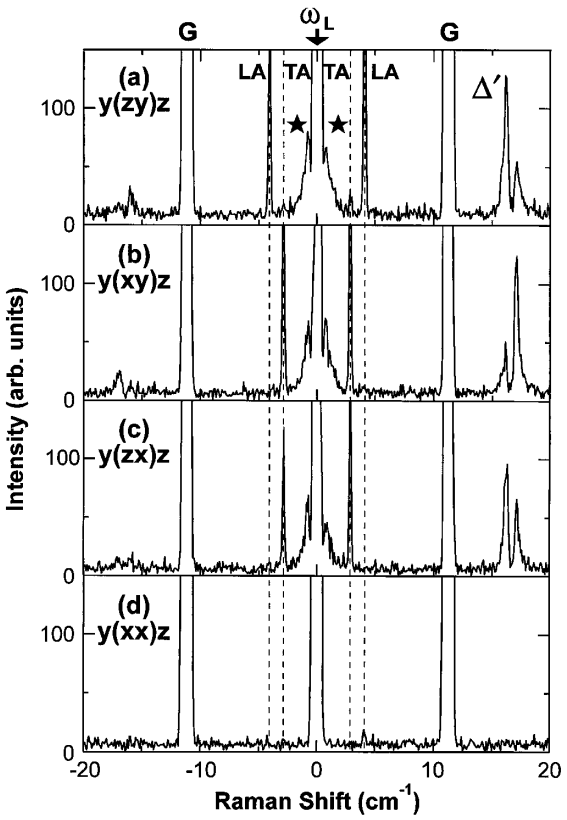

FIG. 3. The Δ' doublet and the star transitions in a man-made type IIb diamond of natural composition studied with the tandem Fabry-Pérot interferometer in a right angle scattering geometry, the incident light being along $\mathbf{y}\|[010]$ and the scattered along $\mathbf{z}\|[001]$. The four panels [(a)–(d)] show the results for four polarization combinations: incident light polarized along $\mathbf{z}$ or $\mathbf{x}\|[100]$ whereas the scattered light is analyzed for $\mathbf{y}$ or $\mathbf{x}$. The exciting wavelength is 5145 Å and the temperature of measurements is 6.0 K.

The splitting in the ^{13}C diamond is observably smaller than that in natural diamond. The average positions of the Jahn-Teller doublets are consistent with our earlier observations [11], i.e., 16.2 cm^{-1} for ^{13}C and 16.7 cm^{-1} for natural composition.

The simplicity of the energy levels involved in the Δ' transition of diamond, observed in a direct manner as an electronic Raman line with cross sections adequate for a high resolution examination, has allowed the Jahn-Teller splitting of the ground state to be clearly detected; the star ($\star$) transition in Figs. 2 and 3 unambiguously and directly confirms it. The large Brillouin shifts of diamond have provided an unobscured spectroscopic view of the "star" transition. Group theoretical arguments in the context of the high site symmetry enable the analysis to be made in a transparent manner. The combination of Raman scattering and group theory have made possible the discovery of the spontaneous lowering of symmetry of a point defect, providing an illustration of the Jahn-Teller theorem in the context of an important material. The present work highlights the power of Raman spectroscopy in its discovery in a most direct fashion.

The authors are grateful to Suresh Vagarali for providing one of the man-made blue diamonds. They acknowledge support from the National Science Foundation Grant No. DMR 98-00858 at Purdue University and from the U.S. Department of Energy, BES Material Sciences (Grant No. W-31-109-ENG-38) at Argonne National Laboratory.

[1] *The Properties of Natural and Synthetic Diamond*, edited by J. E. Field (Academic, London, 1992).
[2] T. R. Anthony, W. F. Banholzer, J. F. Fleischer, L. Wei, P. K. Kuo, R. L. Thomas, and R. W. Pryor, Phys. Rev. B **42**, 1104 (1990); L. Wei, P. K. Kuo, R. L. Thomas, T. R. Anthony, and W. F. Banholzer, Phys. Rev. Lett. **70**, 3764 (1993).
[3] J. C. Angus and C. C. Hayman, Science **241**, 913 (1988). See also A. T. Collins, Semicond. Sci. Technol. **4**, 605 (1989); R. Jackman, Vacuum Solut. **July/August**, 20–23 (1999).
[4] J. F. H. Custers, Physica (Amsterdam) **18**, 489 (1952); **20**, 183 (1954).
[5] In stark contrast, diamonds other than type IIb have resistivities well in excess of 10^{18} Ω cm.
[6] See R. M. Chrenko, Phys. Rev. B **7**, 4560 (1973); E. C. Lightowlers and A. T. Collins, J. Phys. D **9**, 951 (1976).
[7] T. R. Anthony and W. F. Banholzer, Diam. Relat. Mater. **1**, 717 (1992).
[8] See J. R. Hardy, S. D. Smith, and W. Taylor, *The Physics of Semiconductors* (The Institute of Physics and Physical Society, London, 1962), p. 521.
[9] H. Kim, A. K. Ramdas, S. Rodriguez, and T. R. Anthony, Solid State Commun. **102**, 861 (1997).
[10] H. Kim, R. Vogelgesang, A. K. Ramdas, S. Rodriguez, M. Grimsditch, and T. R. Anthony, Phys. Rev. Lett. **79**, 1706 (1997).
[11] H. Kim, R. Vogelgesang, A. K. Ramdas, S. Rodriguez, M. Grimsditch, and T. R. Anthony, Phys. Rev. B. **57**, 15 315 (1998).
[12] This mutual exclusion is strictly true only to the extent parity is a good quantum number.
[13] See, for example, W. Kohn, in *Solid State Physics*, edited by F. Seitz and D. Turnbull (Academic, New York, 1957), Vol. 5, p. 257; J. M. Luttinger, Phys. Rev. **102**, 1030 (1956).
[14] A. K. Ramdas and S. Rodriguez, Rep. Prog. Phys. **44**, 1297 (1981).
[15] J. G. Sandercock, in *Light Scattering in Solids III*, edited by M. Cardona and G. Güntherodt (Springer, Berlin, 1982), p. 173.
[16] H. A. Jahn and E. Teller, Proc. R. Soc. London A **161**, 220 (1937).
[17] T. Matsumoto, O. G. Poluekov, J. Schmidt, E. N. Mokhov, and P. G. Baranov, Phys. Rev. B **55**, 2219 (1997).
[18] V. A. Karasyuk, M. L. W. Thewalt, S. An, and E. C. Lightowlers, Phys. Rev. Lett. **73**, 2340 (1994); V. A. Karasyuk, S. An, M. L. W. Thewalt, E. C. Lightowlers, and A. S. Kaminskii, Solid State Commun. **93**, 379 (1995); V. A. Karasyuk, M. L. W. Thewalt, S. An, E. C. Lightowlers, and A. S. Kaminskii, Phys. Rev. B **54**, 10 543 (1996).